Biomedicine & Pharmacotherapy 186 (2025) 118025

Contents lists available at ScienceDirect

Biomedicine & Pharmacotherapy

journal homepage: www.elsevier.com/locate/biopha

Homoharringtonine (omacetaxine mepesuccinate) limits the angiogenic capacity of endothelial cells and reorganises filamentous actin

Matthias Völkl [a,1], Luisa D. Burgers [b,1], Thomas Josef Zech [a], Sarah Ciurus [b], Senta Dorovska [b], Hong Liu [a], Stefan Zahler [a], Robert Fürst [a,*]

[a] Pharmaceutical Biology, Department of Pharmacy – Center for Drug Research, Ludwig-Maximilians-Universität München, Munich, Germany
[b] Institute of Pharmaceutical Biology, Faculty of Biochemistry, Chemistry and Pharmacy, Goethe University, Frankfurt, Germany

ARTICLE INFO

Keywords:
Homoharringtonine
Endothelial cells
Angiogenesis-related cell functions
Actin cytoskeleton
Rho-associated kinase 1/2
P38/HSP27 axis

ABSTRACT

Homoharringtonine (HHT), an alkaloid from the plant genus *Cephalotaxus*, disrupts the first elongation phase of protein synthesis by interacting with the 60S ribosomal subunit, making it effective in treating diseases such as myeloid leukaemia. Semi-synthetically produced as omacetaxine mepesuccinate, HHT has been approved in Europe and in the US for patients resistant to two or more tyrosine kinase inhibitors. Although recent studies assume an anti-angiogenic capacity, the actions of HHT have not yet been characterised in primary endothelial cells, the major cell type driving angiogenesis. Therefore, this study addresses this issue by investigating the anti-angiogenic effect of HHT *ex vivo* and *in vitro*. A concentration-dependent decrease in sprouting was observed in a mouse aortic ring assay and in spheroids generated from human umbilical vein endothelial cells (HUVECs). Other angiogenic key features such as migration, proliferation and tube formation were similarly decreased by HHT. Interestingly, we observed an accumulation of F-actin. Inhibition of the ROCK pathway restored the angiogenic effects. A specific inhibition of typical upstream or downstream proteins of the ROCK pathway like Rho, MLC-2 or LIMK only marginally restored the angiogenic capability. Further analyses revealed that the alteration of the actin network might relate to the p38 MAPK/HSP27 axis: A significant prolongation of p38 phosphorylation induced by HHT treatment resulted in a partial restoration of endothelial spheroid sprouting. This study demonstrates the anti-angiogenic capabilities of HHT in endothelial cells and opens a promising further research field for an already approved drug.

1. Introduction

The formation of new capillaries from existing blood vessels is called angiogenesis and is of great importance for various physiological processes. Embryonic development, wound healing or the menstrual cycle are prominent examples where angiogenesis is essential for the development and maintenance of life [1,2]. Angiogenesis is tightly regulated by a balance of pro- and anti-angiogenic factors [3,4]. One of the key mediators is the vascular endothelial growth factor (VEGF), which drives angiogenesis and has been identified as a possible therapeutic target already in 1971 [5]. An imbalance in this regulation, often resulting in highly induced angiogenesis, plays a key role in several diseases, including various forms of cancer, rheumatoid arthritis, wet age-related macular degeneration (wAMD) and others [6–8]. Due to this high importance and broad field of therapeutic opportunities, restoring the pro-/anti-angiogenic balance has been the focus of intense scientific effort in the past decades [9–12]. However, due to several drawbacks, such as adverse events, evolving drug resistance or tumour recurrence after treatment, only few drugs with a low therapeutic efficacy have achieved sustained clinical usage [13,14].

Angiogenesis is primarily determined by endothelial cells (ECs) [15]. One driving factor is the remodelling of the actin skeleton of EC [16]. While F-actin is highly important for EC migration, proliferation and vessel maturation [17,18], it has already been shown that a reorganisation of F-actin in ECs can significantly disturb angiogenesis [19,20]. As possible regulatory pathway, the Rho-associated protein kinase (ROCK) was identified in these studies. ROCK is regulated downstream by RhoA, a small GTPase, which in turn is highly important for the cytoskeleton remodelling [21]. ROCK phosphorylates further substrates, including myosin light chain (MLC), MLC phosphatase and LIM kinases (LIMK) [22], and thus mediates the formation of actin stress fibres

* Corresponding author.
E-mail address: robert.fuerst@cup.lmu.de (R. Fürst).
[1] These authors contributed equally to this work and share first authorship

https://doi.org/10.1016/j.biopha.2025.118025
Received 11 November 2024; Received in revised form 25 March 2025; Accepted 27 March 2025
Available online 4 April 2025

Non-standard abbreviations and acronyms

VEGF	Vascular endothelial growth factor
HHT	Homoharringtonine
HUVEC	Human umbilical vein endothelial cells
ROCK	Rho-associated protein kinase
MLC	Myosin light chain
LIMK	LIM kinases
HSP27	Heat shock protein 27
wAMD	Wet age-related macular degeneration
F-actin	Filamentous actin
FAK	Focal adhesion kinase
G-actin	Globular actin
FDA	Food and Drug Administration
TKI	Tyrosine kinase inhibitors
DMSO	Dimethyl sulfoxide
ECGM	Endothelial cell growth medium
FCS	Fetal calf serum
GFR	Growth factor reduced
EC	Endothelial cells
EMA	European Medicine Agency

[23–25]. This increases the stabilisation of actin fibres, which in return reduces the depolarisation of F-actin and thus limits the amount of actin monomers needed for further actin polymerisation, resulting in a reduced cell migration that finally slows down angiogenesis [22,26].

The alkaloid homoharringtonine (HHT) is a natural product derived from species of the plant genus *Cephalotaxus* [27]. HHT hinders mRNA translation by disrupting the first elongation phase of protein synthesis through interaction with the acceptor site on the 60S ribosomal subunit [28,29]. Its pharmacological activity is mainly demonstrated in the treatment of myeloid leukaemia and semi-synthetically produced HHT (omacetaxine mepesuccinate) received approval by the European Medicines Agency (EMA) in 2009 and by the US Food and Drug Administration (FDA) in 2012 for leukaemia patients, for whom treatment with at least two tyrosine kinase inhibitors (TKI) has failed or a resistance has been developed [30]. HHT shows further potential as an anti-inflammatory [31] as well as an anti-angiogenic compound, which was predicted by a pharmacoinformatic study, showing high binding affinity of HHT to the angiogenesis-related proteins VEGF-D, bFGF and MMP-2/9 [32]. HHT in combination with curcumin further showed an inhibition of lymphoma cell growth and angiogenesis via inhibition of the VEGF/Akt signalling pathway as well as an exhibited anti-tumour effect in Raji cells via the VEGF and p-Akt pathway [33]. This prompted us to also investigate putative alternative modes of action of HHT. Surprisingly, the actions of HHT on different key features of angiogenesis have not been systematically investigated to date.

Thus, we analysed HHT for its effects *ex vivo* in an aortic ring assay and *in vitro* by using human umbilical vein endothelial cells (HUVECs) as well-established model for the vascular endothelium. We investigated various steps of angiogenesis like proliferation, migration, tube formation and sprouting from endothelial spheroids and explored a possible pharmacological mechanism behind the effects.

2. Materials and methods

2.1. Compounds

Homoharringtonine (HHT) was purchased from Merck (Darmstadt, Germany), and a stock solution of 10 mM in dimethyl sulfoxide (DMSO, Sigma-Aldrich, St. Louis, MO, USA) was prepared. The Rho inhibitor CT04 (stock solution: 0.1 μg/ml in water) was obtained from Biozol Diagnostics GmbH (Eching, Germany). The ROCK inhibitor Y-27632 (stock solution: 10 mM in DMSO), the LIMK1/2 inhibitor BMS-5 (stock solution: 12 mM in DMSO), the Myosin II inhibitor Blebbistatin (stock solution: 20 mM in DMSO), the MLCK inhibitor peptide 18 (stock solution: 10 mM in water), the p38 MAPK inhibitor SB239063 (stock solution: 10 mM in DMSO) and staurosporine (stock solution: 1 mM in DMSO) were purchased from MedChemExpress (Monmouth, NJ, US). All compounds were stored at −80 °C. For experimental purposes, the stock solutions were freshly diluted without exceeding a final DMSO concentration of 0.1 % (v/v). Recombinant human and murine $VEGF_{165}$ were obtained from PeproTech (Hamburg, Germany) and stored in 100 μg/ml stock solutions resuspended in PBS with 0.1 % BSA.

2.2. Cell culture

Human umbilical vein endothelial cells (HUVECs) were extracted from human umbilical veins as described previously (the research Ethics Committee/Institutional Review Board approved the waiver W1/21Fü for the use of anonymised human material on September 15th, 2021) [34,35]. Cells were grown on plasticware coated with collagen G (10 μg/ml in PBS; Biochrom, Berlin, Germany) up to passage 2 and used for experimental purposes in passage 3. HUVECs were cultivated under constant humidity at 37 °C and 5 % CO_2. EC growth medium (EASY ECGM, PELOBiotech, Planegg/Martinried, Germany) containing 10 % FCS (Biochrom), 100 U/ml penicillin, 100 μg/ml streptomycin (PAN--Biotech, Aidenbach, Germany), 2.5 μg/ml amphotericin B (PAN--Biotech) and a supplement mixture (PELOBiotech) was used as cell culture medium (growth medium). For the starvation of cells, Medium 199 (M199; PAN-Biotech) containing 1 % FCS (Biochrom), 100 U/ml penicillin and 100 μg/ml streptomycin (PAN-Biotech) was utilised (starvation medium).

2.3. Aortic explant culture

Ex vivo animal procedures were performed in compliance with the German Animal Welfare Act (§ 4 Tierschutzgesetz) and approval number V54–19c20/21I-FR/Biologicum, Tierhaus Campus Riedberg (Regierungspräsidium Darmstadt, Germany). The *ex vivo* animal experiments were conducted using 4- to 6-week-old C57BL/6 N mice, which were kept under a 12-h/12-h light/dark cycle and had access to food and water ad libitum until sacrifice. Mouse aortic ring assays were performed as previously described [36,37]. 4- to 6-week-old C57BL6/N mice were used, which were kindly provided by the group of Prof. Achim Schmidtko (Institute of Pharmacology and Clinical Pharmacy, Goethe University Frankfurt, Frankfurt, Germany). Briefly, mice were sacrificed using CO_2 followed by subsequent cervical dislocation to ensure death. Next, the aortae were explanted, surrounding tissue was removed, and the explants were cut into rings of about 0.5–1 mm length. These rings were then incubated overnight in Opti-MEM I (Gibco/Thermo Scientifc, Waltham, Massachusetts, USA) supplemented with 100 U/ml penicillin and 100 μg/ml streptomycin (P/S; Pan-Biotech). On the following day, rings were embedded into a rat tail collagen I gel (1.5 mg/ml in M199; Corning, Corning, New York, USA) and incubated with Opti-MEM I supplemented with P/S, 2.5 % FCS Superior (Sigma-Aldrich), and 30 μg/ml murine vascular endothelial growth factor (mVEGF165; PeproTech) until first endothelial sprouts were visible (3–5 days). Sprouting rings were subsequently treated with 100 nM HHT or vehicle control for 3 additional days. Subsequently, the treatment was terminated by fixating the rings with ROTI-Histofix (Carl Roth, Karlsruhe, Germany) for 30 min. Next, the rings were permeabilised using 0.25 % Triton X-100 (Carl Roth) twice at room temperature. To block unspecific binding, the rings were incubated in 1 % BSA (Carl Roth) in PBS at 4 °C overnight. Afterwards, staining with FITC-coupled BS-I Lectin (L9381, 0.1 mg/ml, Sigma-Aldrich) and a CY3-conjugated antibody against smooth muscle actin (α-SMA, C6198, Dilution 1:1000, Sigma-Aldrich) was performed at 4 °C overnight. After thorough washing of the rings with 0.1 % Triton X-100, images were taken using a confocal laser

scanning microscope (LSM 780, Zeiss), and sprouting was quantified manually using Fiji/ImageJ (version 1.53 t, NIH).

2.4. Spheroid sprouting

EC-derived spheroids were created by using the hanging drop method as described previously with slight modifications [37]. In brief, HUVECs were dispensed in growth medium containing methylcellulose (0.25 %, Sigma-Aldrich) and seeded to square Petri dishes. After 24 h, the spheroids were embedded in a collagen gel, pretreated for 30 min with HHT and sprouting was induced by recombinant human $VEGF_{165}$ (10 ng/ml). Where indicated, CT04 (0.03–0.1 μg/ml), Y-27632 (10 μM), BMS-5 (1 μM), Blebbistatin (3 μM), MLCK inhibitor peptide 18 (10 μM) or SB239063 (10 μM) was added to the embedded spheroids 30 min before HHT treatment. After a total time of 20 h, microscopical images were taken with a Leica DM IL LED inverted microscope (Leica Microsystems, Wetzlar, Germany). Total sprout length and number of sprouts per spheroids were analysed using ImageJ (version 1.53 t, NIH).

2.5. Network formation

For the analysis of endothelial network formation, angiogenesis μ-slides (ibidi, Gräfelfing, Germany) were used. The slides were coated with growth-factor-reduced (GFR) Matrigel (Corning). HUVECs (8.5×10^3 cells) were seeded to the Matrigel and treated with HHT. Where indicated, CT04 (0.03–0.1 μg/ml), Y-27632 (10 μM), BMS-5 (1 μM), Blebbistatin (3 μM), MLCK inhibitor peptide 18 (10 μM) or SB239063 (10 μM) was added to the HUVECs 30 min before HHT treatment. After 6 h of network formation, images were taken with a Leica DM IL LED inverted microscope (Leica Microsystems). The ImageJ plugin "Angiogenesis analyzer" was used to quantify the characteristics "number of junctions", "total branching length" and "number of tubules".

2.6. Cell migration

The undirected migration of HUVECs was analysed using a scratch assay. A scratch was inflicted to a confluent layer of HUVECs using a pipette tip, and the cells were treated with HHT as indicated. HUVECs were allowed to migrate until the gap in the vehicle-treated control cells was closed (100 % migration). HUVECs treated with starvation medium served as negative control representing 0 % migration. Where indicated, CT04 (0.03–0.1 μg/ml), Y-27632 (10 μM), BMS-5 (1 μM), Blebbistatin (3 μM), MLCK inhibitor peptide 18 (10 μM) or SB239063 (10 μM) was added to the scratched HUVEC monolayers 30 min before HHT treatment. The relative migration in relation to the starvation control was analysed using a Leica DM IL LED inverted microscope (Leica Microsystems) and ImageJ (version 1.53 t, NIH).

The chemotactic migration of HUVECs was assessed using a Boyden chamber experiment. HUVECs (1×10^5) were allowed to adhere to Transwell inserts (8 μm pore size, polycarbonate; Corning) coated with collagen G (10 μg/ml; Biochrom) for 4 h. Subsequently, HHT at the indicated concentrations was added to the Transwell system, and a chemotactic gradient (20 % FCS; Biochrom) was applied. HUVECs were allowed to migrate through the Transwell insert towards the chemoattractant for 16 h. Migrated cells were fixed with 4 % formaldehyde (Roti-Histofix; Carl Roth) and stained with crystal violet (0.5 % crystal violet in 20 % methanol). After complete drying, crystal violet was solubilised with 20 % acetic acid in water. Absorbance was measured at 540 nm using a microplate reader (Infinite F200 Pro, Tecan, Männedorf, Switzerland).

For live-cell imaging of single cells in a chemotactic gradient, μ-Slide Chemotaxis Chambers (ibidi) were used according to the manufacturer's instructions. HUVECs were treated as indicated with HHT, and a stable linear concentration gradient (0–20 % FCS) was established. HUVECs were observed for 20 h in a climate chamber (37 °C, 5 % CO_2). Images of migrating cells were taken every 10 min with a Leica DMI6000 B fluorescence microscope (Leica Microsystems). The ImageJ plugins "Manual Tracking" and "Chemotaxis Analysis" were used to analyse migration (version 1.53 t, NIH).

2.7. Cell proliferation

HUVECs (3×10^3) were cultured for 24 h in 96-well plates and then treated as indicated with HHT for 48 h. Cells were fixed with a methanol/ethanol solution (2:1 v/v) and stained with crystal violet (0.5 % crystal violet in 20 % methanol). After complete drying, crystal violet was solubilised with 20 % acetic acid in water. Absorbance was measured at 540 nm using a microplate reader (Infinite F200 Pro, Tecan).

2.8. Flow cytometry

For measurement of BrdU incorporation, 4.4×10^4 HUVECs were grown for 24 h and then serum-starved for 8 h to synchronize all cells in the G_0/G_1 phase of the cell cycle. HUVECs were then treated with HHT in growth medium for a total time of 24 h. 10 μM BrdU (Sigma-Aldrich) was added to the HUVECs 8 h before the treatment end point. Cells were detached using trypsin/EDTA (Biochrom), washed with cold PBS and fixed in absolute ethanol for 96 h at 4 °C. Treatment with 2 N HCl/Triton X-100 (Sigma-Aldrich) for 30 min at room temperature was performed to denature the DNA. Samples were then washed with 0.1 M $Na_2B_4O_7$ (pH 8.5; Sigma-Aldrich) for neutralisation and incubated overnight at 4 °C with a FITC-labelled anti-BrdU antibody (Becton Dickinson, Heidelberg, Germany). BrdU incorporation was analysed by recording median values for 3000 events per sample using a FACSVerse flow cytometer (BD Bioscience, Heidelberg, Germany).

For cell cycle analysis, 4.4×10^4 HUVECs were grown for 24 h and then treated with HHT as indicated for 24 h. HUVECs were detached using trypsin/EDTA (Biochrom) and washed with cold PBS. HUVECs were incubated overnight at 4 °C with a staining solution (50 μg/ml propidium iodide (Sigma-Aldrich), 1 % Triton X-100 (BD Bioscience), 1 % sodium citrate (Carl Roth) in PBS). Cell cycle distribution was analysed using a FACSVerse flow cytometer (BD Bioscience).

2.9. Western blot analysis

HUVECs were treated as indicated and then lysed with RIPA lysis buffer containing protease and phosphatase inhibitors. The protein content of each sample was quantified using the Pierce BCA Protein Assay Kit (Thermo Fisher Scientific). A pyronin-based sample buffer containing sodium dodecyl sulphate (SDS; BD Bioscience) was added to the samples, which were then incubated at 95 °C for 5 min. Equal amounts of protein (range: 20–40 μg) were separated by SDS-polyacrylamide gel electrophoresis (SDS-PAGE; Bio-Rad Laboratories, Hercules, California, USA). The proteins were transferred to a polyvinylidene fluoride membrane (PVDF; Bio-Rad Laboratories,) by semi-dry electroblotting (Trans-Blot Turbo Transfer System, Bio-Rad Laboratories). Unspecific binding sites were blocked with 5 % non-fat dry milk (Blotto; Carl Roth) or 5 % BSA (MilliporeSigma, St. Louis, Missouri, USA) containing 0.1 % Tween-20 (Sigma-Aldrich). The following primary antibodies were used: rabbit anti-human phospho-MLC2 (p-MLC2, 1:2000; #3674), rabbit anti-human MLC2 (1:1000; #3672), rabbit anti-human ROCK1 (1:1000; #4035), rabbit anti-human ROCK2 (1:1000; #47012), rabbit anti-human phospho-ezrin/radixin/moesin (p-ERM, 1:1000; #3141), rabbit anti-human ezrin/radixin/moesin (ERM, 1:1000; #3142), rabbit anti-human phospho-p38 (p-p38, 1:1000; #9212), rabbit anti-human p38 (1:2000; #4511), rabbit anti-human β-tubulin (1:1000; #2128), rabbit anti-human phospho-HSP27 (1:2000; #9709), mouse anti-human HSP27 (1:2000; #2402), goat anti-rabbit linked to HRP (1:3000; #7074) and goat anti-mouse linked to HRP (1:3000; #7076). Antibodies were obtained from Cell Signalling

(Frankfurt am Main, Germany). Mouse anti-human β-actin-peroxidase (loading control, 1:100.000, A3854) was obtained from Sigma Aldrich (St. Louis, Missouri, USA). Protein expression was detected by chemiluminescence measurement. Quantification of protein expression was performed by densitometric analysis of protein bands using ImageJ (version 1.53 t, NIH).

2.10. Immunofluorescence staining

HUVECs were grown to confluence on 8-well μ-slides (ibidi) and treated as indicated. Subsequently, the cells were fixed with 4 % formaldehyde (Roti-Histofix; Carl Roth) and permeabilised with 0.2 % Triton X-100 (Sigma-Aldrich). Unspecific binding sites were blocked with 0.2 % BSA (MilliporeSigma) for 30 min. F-actin fibres were stained using rhodamine phalloidin (1:400; R415, Thermo Fisher Scientific). Cell nuclei were visualised with Hoechst 33342 (1 μg/ml; Sigma-Aldrich). Immunofluorescence images were captured with a Leica DMI6000B fluorescence microscope (Leica Microsystems).

2.11. Statistical analysis

Different donors of primary cells represent independently performed experiments (*n*). All experiments were performed independently at least three times; the respective figure legends contain the actual number of independently performed experiments. Statistical analyses were performed using the GraphPad Prism software version 10.0 (Dotmatics, Boston, Massachusetts, USA). Statistically significant differences ($p \leq 0.05$) were evaluated by one-way ANOVA followed by Tukey's *post hoc* test or Mann-Whitney *U* test. Data are expressed as mean ± standard error of the mean (SEM).

3. Results

3.1. Homoharringtonine inhibits angiogenic key features ex vivo and in vitro

To exclude the possibility that pharmacological effects of HTT are a consequence of cytotoxicity, the cytotoxic concentrations of HHT for ECs have recently been determined by our group [31]. Treating HUVECs

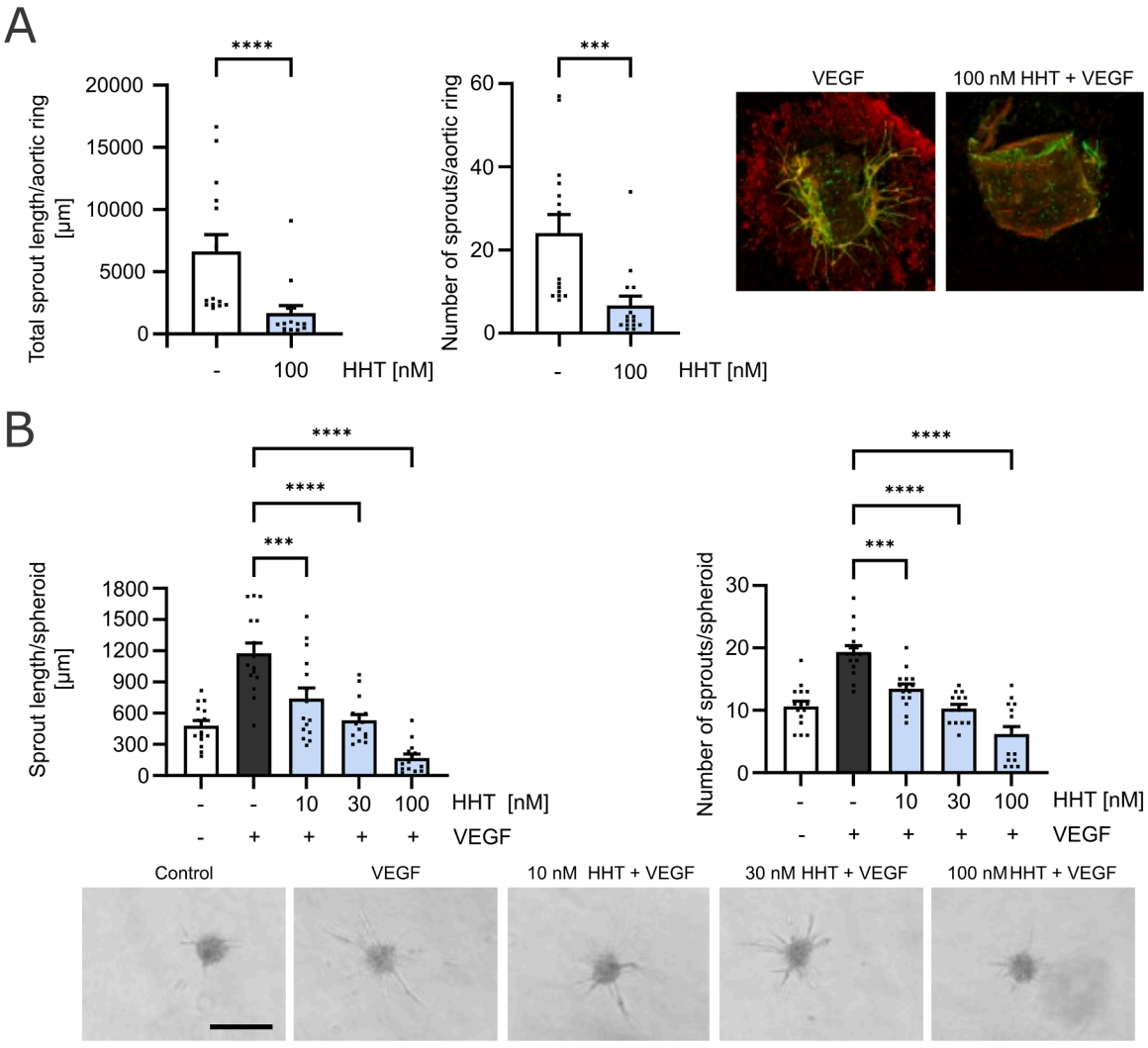

Fig. 1. HTT suppresses VEGF-induced angiogenic events both *ex vivo* and *in vitro*. A: Analysis of mVEGF (30-μg/ml)-activated mouse aortic rings treated for 3 days with 100 nM HHT; total length of sprouts per ring (left) and number of sprouts per ring (middle). Representative images of aortic rings stained with fluorescent BS I lectin (green) and a fluorescent anti-α-SMA antibody (red) after treatment (right). B: HUVEC spheroids were pre-incubated with VEGF (10 ng/ml) for 30 min and then treated for 20 h with HHT; Analysis of total length of sprouts per spheroid (left) and number of sprouts per spheroid (right). Representative images of collagen-embedded HUVEC spheroids at the end of treatment (below, scale bar = 400 μm). Data represent the mean ± SEM, n = 3 mice (a) or 3 donors (b); *** $p \leq 0.001$, **** $p \leq 0.0001$ analysed by one-way ANOVA followed by Tukey's post hoc test.

for 24 hours with concentrations of up to 300 nM HHT showed no impact on typical viability markers such as the metabolic activity (CellTiter-Blue assay), the membrane integrity (lactate dehydrogenase assay) and apoptosis (subdiploidic DNA content). Therefore, as a precautionary measure for all subsequent experiments, a maximal treatment concentration of 100 nM was selected for the analysis of the anti-angiogenic capacity of HHT. A first insight into the anti-angiogenic capacity of HHT was determined by an *ex vivo* aortic ring assay (Fig. 1A). Mouse thoracic aortic rings allow for a specific and isolated investigation of angiogenic growth behaviour, while still maintaining a close mimicry of physiological angiogenesis [36]. HHT showed a significant decrease in sprouting length and number of sprouts per aortic ring (average control vs. HHT: 6628 µm: 1651 µm; 24.1 sprouts: 6.7 sprouts) compared to a VEGF-treated control.

Subsequently, an *in vitro* 3D sprouting assay utilising HUVEC-derived spheroids (Fig. 1B) was performed. Spheroids sprouting was induced by adding 10 ng/ml VEGF. The VEGF-induced sprouting length was reduced concentration-dependently from 1176 µm to 169 µm by 100 nM HHT. The reduction in the number of sprouts per spheroid from 19.3 to 6.2 followed the same concentration-dependent behaviour. Both parameters were reduced even below the negative control level (sprouting length = 480 µm, number of sprouts per spheroid 10.6). Since both, *in vitro* and *ex vivo* data showed a strong anti-angiogenic capacity of HHT, a more profound analysis was performed.

One key feature of angiogenesis is the migratory behaviour of EC. By inflicting a scratch in a confluent HUVEC monolayer, the undirected migration was measured by analysing the covered area of the scratch (Fig. 2A). Here, treatment with 100 nM of HHT reduced the coverage concentration-dependently by up to 47 % compared to the untreated control.

Next, the directed migration towards a chemotactic stimulus was determined. A Boyden chamber assay with a 20 % FCS gradient was performed (Fig. 2B). Consistent with the observed effect on the undirected migration, HHT significantly reduced about half of the serum-induced migration compared to the untreated cells. To further elucidate the influence of HHT on the characteristics of chemotactic migration of HUVEC cells towards an FCS gradient, we additionally performed live-cell imaging experiments using µ-Slide Chemotaxis chambers. Again, all key features showed a significant decrease in migration after HHT treatment compared to the control (Fig. 2C). Both the directional and overall motility were significantly reduced by HHT.

In addition to cell migration, proliferation is an important step in the formation of new blood vessels, especially for the prolongation and stabilisation of newly formed sprouts [38]. By using a crystal violet staining-based proliferation assay, we observed an effective, concentration-dependent reduction in proliferation of HUVECs over a 48-hour timeframe (Fig. 3A). Notably, a concentration of 100 nM HHT already completely halted cell proliferation. This proliferation inhibition aligns with the ability of HHT to hinder the incorporation of BrdU nearly entirely into newly synthesised DNA (Fig. 3B). Using flow cytometry, the cell cycle in HUVECs treated with HHT was additionally analysed. Hereby, a significant decrease of cells in the G2-phase after 24 h of HHT treatment was observed, accompanied by a coherent increase in the percentage of cells in the G0/G1- and S-phase (Figure S1). Finally, a tube formation assay with HUVECs seeded on top of GFR Matrigel was conducted (Fig. 3C). The reoccurring pattern of the anti-angiogenic potential of HHT could be observed here as well. Junction number, branching length as well as tubules number significantly decreased after 6 h of HHT treatment in a concentration-dependent manner. Overall, HHT treatment leads to a notable reduction in all studied angiogenic key features of ECs i.e. sprouting, migration, proliferation, and the ability to form a tube network.

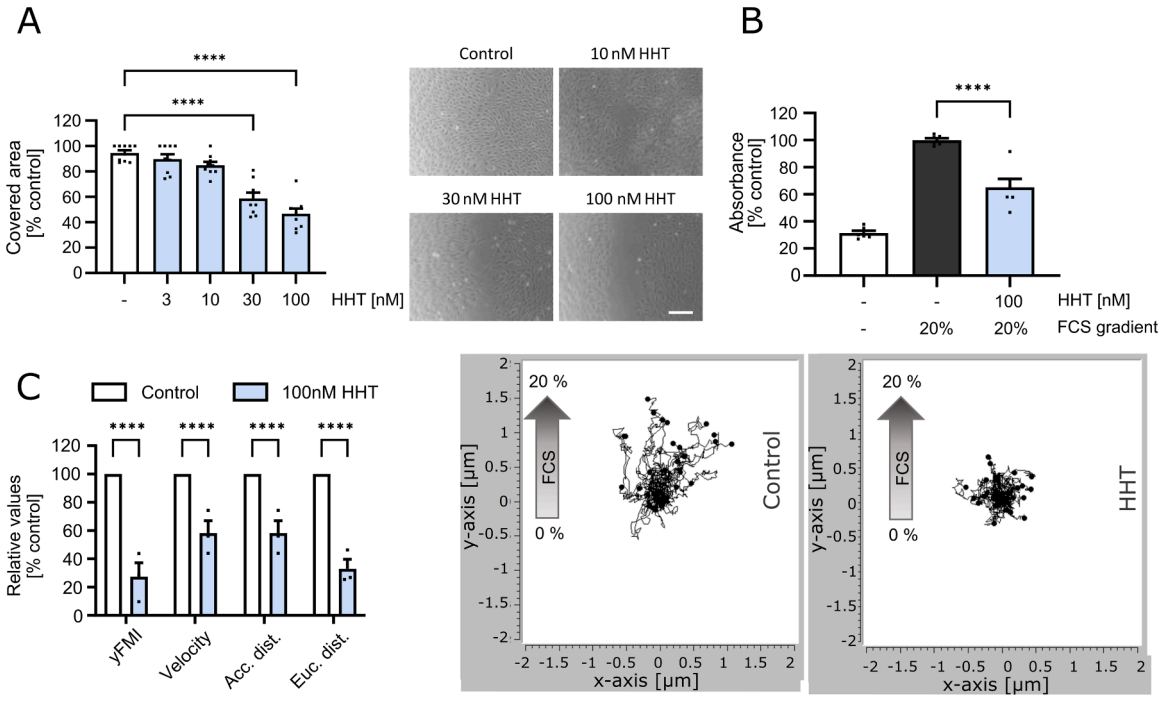

Fig. 2. HHT inhibits undirected and directed migration in HUVECs. A: HUVECs were grown to confluency, a scratch was inflicted, cells were treated with HHT as indicated and the cells were allowed to migrate until the untreated control cells had closed the scratch again. The covered area was analysed using ImageJ software. Scale bar represents 200 µm. B: HUVECs were grown on Transwell inserts (pore size 8 µm) until confluence and then treated with HHT as indicated. Cells were allowed to migrate towards a chemotactic gradient (20 % FCS) for 16 h and were subsequently stained with crystal violet solution. Absorbance was measured at 540 nm. C: The migration of HUVECs in response to a 20 % FCS chemotactic gradient was assessed using µ-Slide Chemotaxis chambers. Cells were either left untreated (control) or treated with 100 nM HHT. The cells were tracked for 20 h, and the data was analysed using the "Manual Tracking" and "Chemotaxis Analysis" plugins in ImageJ. Data represent the mean ± SEM, n = 3 donors; *** $p \leq 0.001$, **** $p \leq 0.0001$ analysed by one-way ANOVA followed by Tukey's post hoc test.

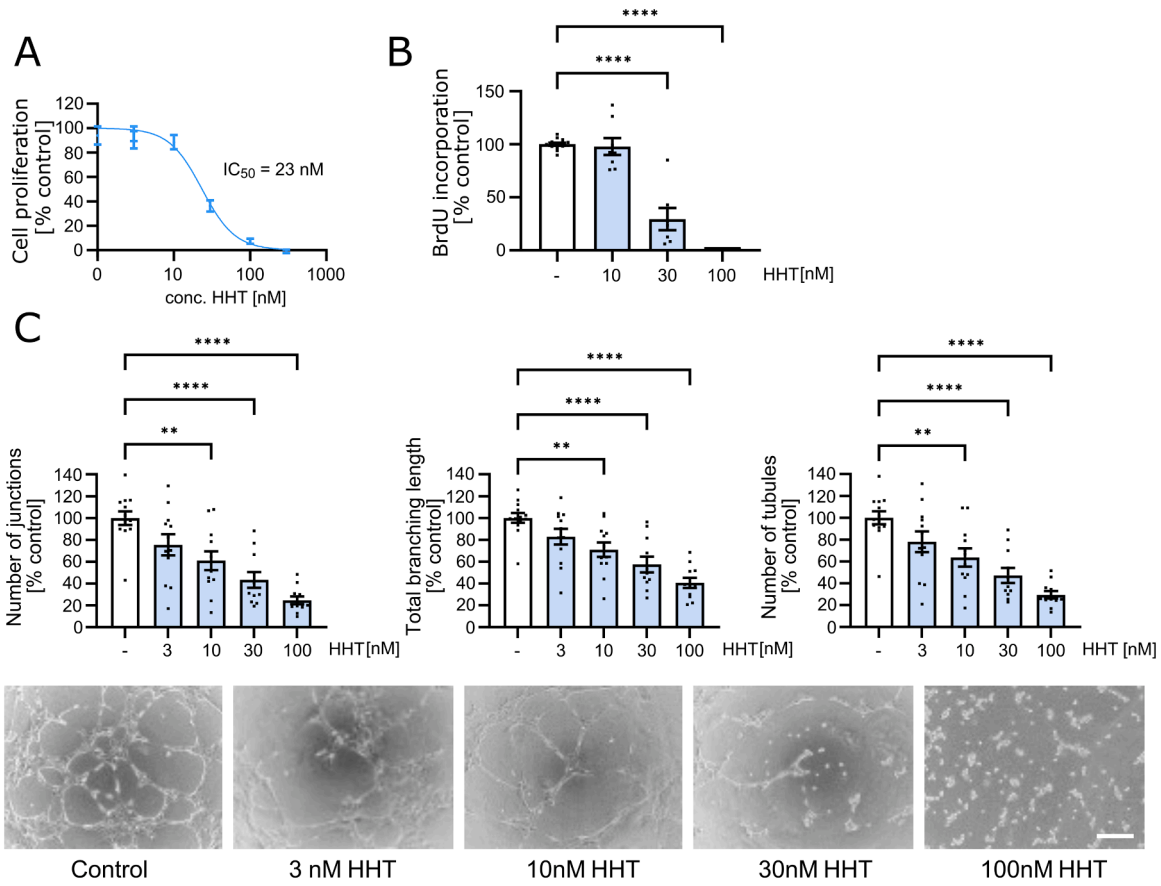

Fig. 3. HHT inhibits proliferation and tube formation in HUVECs. A: HUVECs were cultured at low density for 24 h, treated with HHT as specified for 48 h, and then stained with crystal violet solution. Absorbance was measured at 540 nm. B: HUVECs were cultured at low density for 24 h, serum-starved, and subsequently treated with the indicated concentrations of HHT for 24 h in growth medium. BrdU (10 μM) was added to the cells 8 h before the treatment endpoint. The relative amount of incorporated BrdU was determined using flow cytometry. C: HUVECs were cultured on, with GFR Matrigel pre-coated, μ-slides and treated for 6 h with HHT as indicated and representative picture were taken. Network formation was analysed by ImageJ; Scale bar = 50 μm. Data represent the mean + SEM, n = 3 donors; ** $p \leq 0.01$, *** $p \leq 0.001$, **** $p \leq 0.0001$ analysed by one-way ANOVA followed by Tukey's post hoc test.

3.2. Inhibition of the ROCK pathway restores some effects of homoharringtonine

We have recently shown that protein biosynthesis inhibitors (structurally unrelated to HHT) are capable of altering the actin cytoskeleton [19,20]. Since actin is related to proliferation, migration and angiogenesis [39], we examined the influence of HHT on the actin cytoskeleton by staining F-actin in HUVECs: In fact, HHT treatment for 24 h led to an increase of F-actin by 27 % (Fig. 4A) in a confluent HUVEC monolayer. This accumulation of actin stress fibres is likely to have a responsibility for the anti-angiogenic effects. One of the key signalling pathways in the regulation of the actin cytoskeleton depends on ROCK. Therefore, we repeated the F-actin staining and the functional assays (sprouting, migration and tube formation) in presence of the potent ROCK inhibitor Y-27632 (Fig. 4A/B). Indeed, a pre-incubation with the inhibitor mitigated the effects of HHT almost to control level. Interestingly, an inhibition of the Rho proteins, which are known ROCK activators, by the Rho inhibitor CT04, had no impact on the effects of HHT (Figure S2). Additionally, we analysed other upstream regulators of the ROCK pathway, like Akt or focal adhesion kinase (FAK). However, no significant increase or prolongation of the the phosphorylation of Akt or FAK could be observed by western blotting (data not shown). This suggests that HHT causes its effects *via* ROCK but independently of Rho, Akt or FAK.

It therefore seemed likely that the effects of HHT were caused by downstream proteins of the ROCK pathway. Especially MLC-2 and LIMK, which are responsible for stress fibre assembly and contraction (MLC) or F-actin stabilisation (LIMK), influence the formation of the actin skeleton [40]. We inhibited LIMK1/2 with the selective inhibitor BMS-5 and MLC-2 with the myosin-II-inhibitor Blebbistatin: While the inhibition of LIMK1/2 had no effect on the HHT-evoked effects on sprouting, migration and tube formation (Fig. 5A), inhibition of myosin II by Blebbistatin partially restored effects (Fig. 5B). Interestingly, when inhibiting only MLCK, the effects of HHT on sprouting and tube formation were not influenced, and only a small rescue effect on cell migration was observed (Fig. 5C).

This led to the conclusion that if HHT effects the cells *via* the ROCK pathway, only the ROCK/myosin axis is involved. To further analyse the influence of HHT on the ROCK pathway, we investigated the cleavage, and therefore activation, of ROCK1. While a treatment of HUVECs with staurosporine (100 nM) for 4 h led to a significant increase in ROCK1 cleavage and thus its activation, HHT had no effect on either the cleavage of ROCK1 or the total protein level of uncleaved ROCK1 over 24 h (Figure S3). HHT also had no effect on the phosphorylation of MLC-2, while staurosporine as control strongly reduced MLC-2 phosphorylation. In addition to ROCK1, ROCK2 can also exert effects on angiogenic processes and the actin network by activating the ERM (ezrin/radixin/moesin) proteins. However, as observed for ROCK1, HHT had no effect on the protein level of ROCK2 or on the basal activation of ERM proteins (Figure S4). This suggests that HHT exerts its effects by altering the actin network, since inhibition of F-actin formation by ROCK inhibition abolished the effects. However, specific inhibition of the ROCK pathway did only partly reverse the effects of HHT, suggesting that the alterations of the actin cytoskeleton seem to depend on other effects as well.

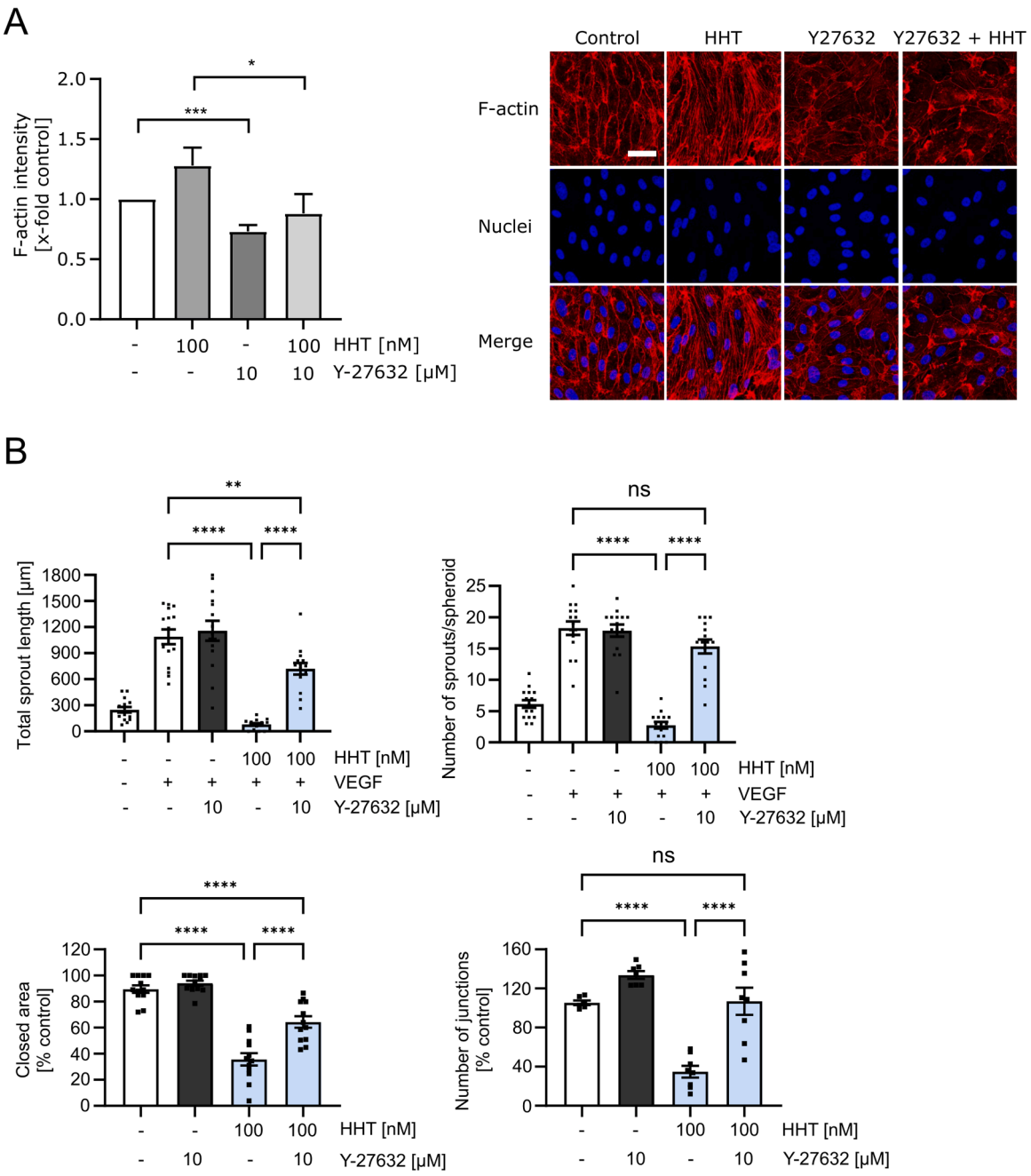

Fig. 4. Actin accumulation due to HHT treatment and effect of the ROCK inhibitor Y-27632. A: HUVECs were grown to confluence on 8-well µ-slides, and HHT was added for 24 h. Where indicated, Y-27632 was added 30 min before HHT treatment. F-actin was stained using rhodamine phalloidin (red), cell nuclei with Hoechst 33342 (blue). B: Sprouting length and number of VEGF (10 ng/ml) pre-stimulated (30 min) HUVEC spheroids were determined. Where annotated, spheroids were additionally treated for 20 h with HHT. For the undirected migration, HUVECs were grown to confluency, a scratch was inflicted, cells were treated with HHT as indicated and the cells were allowed to migrate until the untreated control cells had closed the scratch. For tube formation and analysis of the junction number, HUVECs were cultured on pre-coated µ-slides and treated for 6 h with HHT as indicated. Where indicated, Y-27632 was added 30 min before HHT treatment. Data was analysed by ImageJ and represent the mean + SEM, n = 3 donors; * $p \leq 0.05$, ** $p \leq 0.01$, *** $p \leq 0.001$, **** $p \leq 0.0001$ analysed by one-way ANOVA followed by Tukey's post hoc test.

3.3. Homoharringtonine exerts its effects partly via the p38/HSP27 axis

One possibility is hereby the phosphorylation of HSP27, which binds to actin and shifts the balance towards more F-actin. This phosphorylation step is promoted by the activation of p38 [41] which our group has recently shown that HHT activates [31]. We therefore hypothesised that this might be the process which regulates F-actin in our setting. In fact, HHT led to a strongly prolonged activation of the VEGF-induced p38 activation from 15 min to 16 h (Fig. 6A). Moreover, pre-incubation of the cells with the p38 inhibitor SB239063 led to a reduction in the HHT-evoked F-actin stress fibre formation (Fig. 6B). In agreement with these results, HHT also extended the VEGF-induced phosphorylation of HSP27 from about 1 h to at least 8 h (Fig. 6C). After addition of the p38 inhibitor SB239063, VEGF/HHT-induced HSP27 phosphorylation was significantly reduced after 30 min, indicating that p38 is indeed involved in the HHT-triggered phosphorylation of HSP27. In terms of influencing the angiogenic processes in HUVECs, the inhibition of p38 led to a significant restoration of HHT-reduced

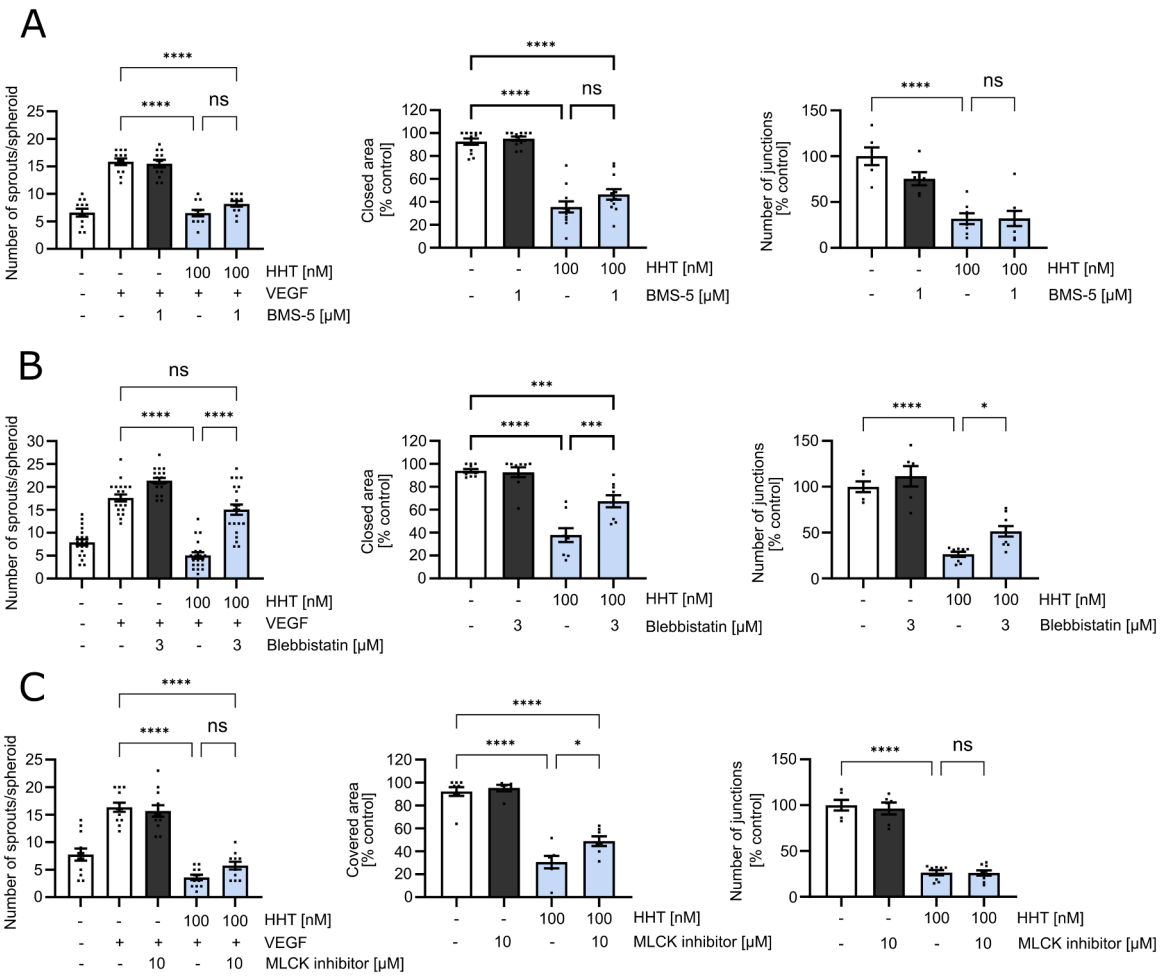

Fig. 5. Inhibition of MLC-2 and LIMK 1/2 only partly restores angiogenic key features. A: Analysis of sprouts per spheroid in VEGF (10 ng/ml) pre-activated (30 min) HUVEC spheroids treated for 20 h with HHT. For the undirected migration, HUVECs were grown to confluency, a scratch was inflicted, cells were treated with HHT as indicated and the cells were allowed to migrate until the untreated control cells had closed the scratch. For tube formation and analysis of the junction number, HUVECs were cultured on μ-slides pre-coated with GFR Matrigel and treated for 6 h with HHT as indicated. Where indicated, BMS-5 (A), Blebbistatin (B) or the MLCK inhibitor (C) were added 30 min before HHT treatment. Data was analysed by ImageJ and represent the mean + SEM, n = 3 donors; * $p \leq 0.05$, ** $p \leq 0.01$, *** $p \leq 0.001$, **** $p \leq 0.0001$ analysed by one-way ANOVA followed by Tukey's post hoc test.

sprouting. Surprisingly though, inhibition of p38 had no effect on migration or tube formation (Fig. 6D). Overall, the experiments suggest that HHT exerts its effects, at least in part, via an increase of F-actin and that this is associated with an enhancement of the p38/HSP27 axis.

4. Discussion

Angiogenesis, the formation of new capillaries from existing blood vessels, is a crucial process for the development and maintenance of life and is regulated by a balance of pro- and anti-angiogenic factors [1,2]. Imbalances in this tightly controlled process can lead to or drive various diseases like cancer, rheumatoid arthritis or wAMD [9–12]. Therefore, targeting angiogenesis is a clinically established and valuable therapeutic approach. However, despite scientific advances, various challenges such as adverse events and drug resistance persist [14], which warrants the search for novel treatment options.

HHT is approved as back-up medication for myeloid leukaemia if treatment with two or more tyrosine kinase inhibitors has failed [42]. In cancer cells, HHT has already been shown to supress migration or proliferation, two important cell functions related to angiogenesis [43–46]. Further indications for an anti-angiogenic capacity where made e.g. in lymphoblast cells (K562), in a epithelial cell line previously considered as endothelial (ECV304) [47] and in lymphoma cells (U937 and Raji cells) [33], in which HHT down-regulates VEGF expression. Prome et al. (2023) identified HHT as a promising candidate using a reverse docking approach to investigate the anticancer potential of natural compounds, specifically targeting metastasis and angiogenesis. [32]. Surprisingly, however, there are no data on primary ECs, despite the fact ECs are the main drivers of angiogenesis [48].

In our work, HHT indeed showed a potent anti-angiogenic capacity *ex vivo* in an aortic ring assay and *in vitro* in a spheroid sprouting model. *In vitro* studies with HUVECs revealed a notable reduction in all studied angiogenic key functions like migration, proliferation, and the ability to form tube like structures, likely caused by an increase of F-actin.

As described above, it has already been shown that HHT down-regulates VEGF expression [33,47]. Here, we additionally showed a concentration-dependent decrease in VEGF-induced angiogenesis for primary ECs. HHT treatment resulted in a significant decrease of spouting of spheroids and aortic rings, even below control level, proving the potent anti-angiogenic capability of HHT. Angiogenesis is not only driven by a VEGF-activated endothelium, but a multi-step process involving migration, proliferation, and the formation of endothelial tubes. While other research on HHT regarding migration and proliferation with cancer cell lines like RAW264.7 [49], glioblastoma cells [50] or hepatocellular carcinoma [51] already showed a decrease of these cell functions after HHT treatment, we showed inhibition of migration

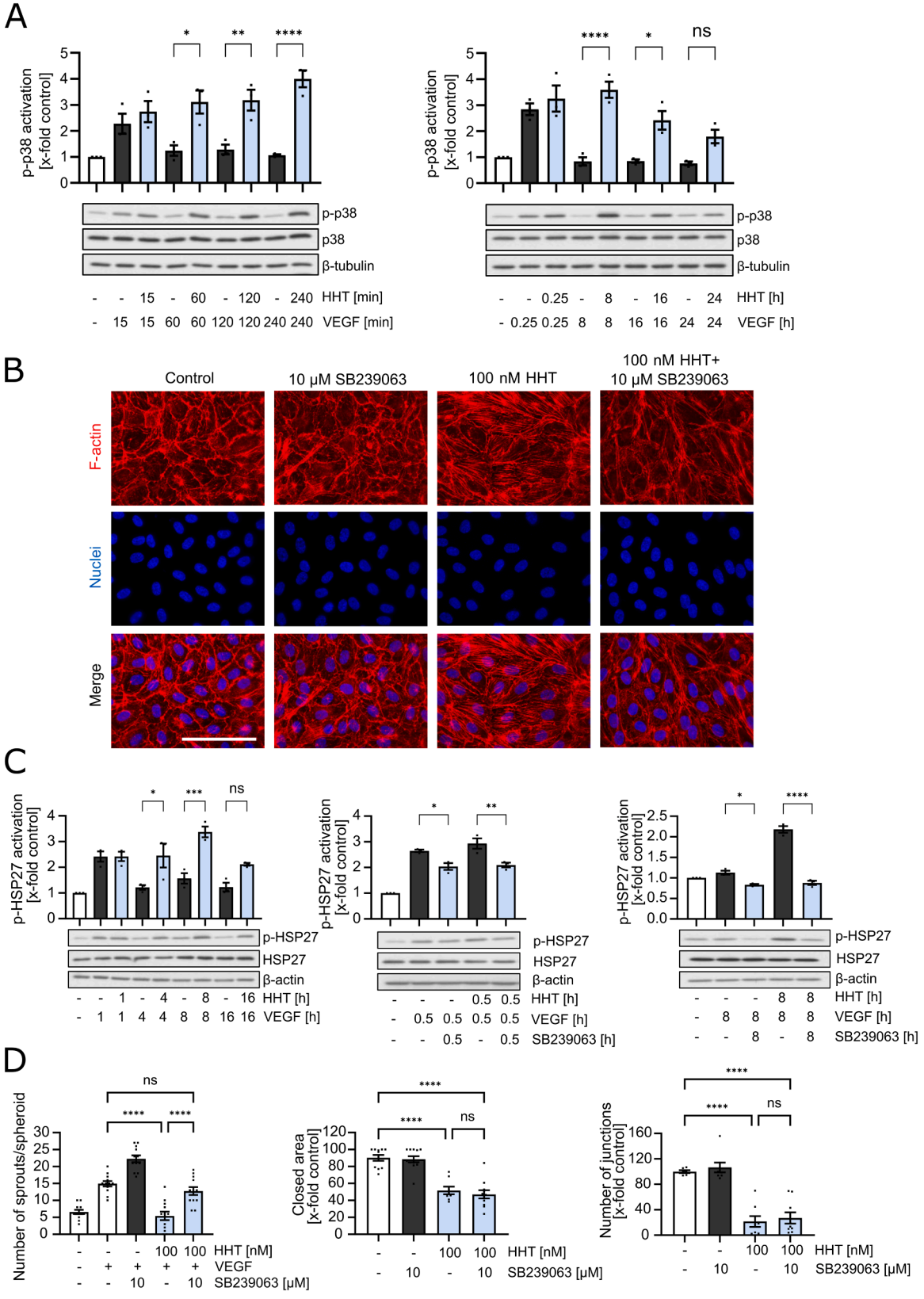

(caption on next page)

Fig. 6. HHT prolongs p38-dependent HSP27 signalling, which partly causes the observed anti-angiogenic effects. A: Confluent HUVECs were treated with 100 nM HHT as indicated. Total protein levels of p38 and phospho-p38 (p-p38) were determined by western blot analysis. B: Immunostaining of a confluent HUVEC layer, Cells were pre-incubated with SB239063 for 30 min and subsequently 100 nM of HHT was added for 24 h. F-actin was stained by rhodamine phalloidin (red) and cell nuclei by Hoechst 33342 (blue), scale bar 50 μm C: Confluent HUVECs were treated with 10 ng/ml VEGF, 100 nM HHT and 10 μM SB239063 as indicated. Total protein levels of HSP27 and phospho-HSP27 (p-HSP27) were determined by western blot analysis. D: Key functional experiments were performed in HUVECs treated with a combination of HHT and SB23063. Length and number of sprouts was determined. Spheroids were pre-treated for 30 min with HHT and then stimulated with VEGF (10 ng/ml for 20 h (left)). For the undirected migration, HUVECs were grown to confluency, a scratch was inflicted, cells were treated with HHT as indicated and the cells were allowed to migrate until the untreated control cells had closed the scratch (middle). For tube formation and analysis of the junction number, HUVECs were cultured on pre-coated μ-slides and treated for 6 h with HHT as indicated (right). Where indicated, SB239063 was added 30 min before HHT treatment. Data was analysed by ImageJ and represent the mean + SEM, n = 3 donors; * $p \leq 0.05$, ** $p \leq 0.01$, *** $p \leq 0.001$, **** $p \leq 0.0001$ analysed by one-way ANOVA followed by Tukey's post hoc test.

and proliferation for the first time in primary ECs. By targeting both, the proliferation of the ECs themselves as well as their capability to form new blood vessels by inhibiting the migration and tube formation, HHT presents a broad approach to inhibit angiogenesis. Interestingly, a recent study from our lab showed that HHT also exerts anti-inflammatory effects [31]. In certain diseases, such as wAMD, despite the use of angiogenesis inhibitors, disease progression remains driven by inflammatory processes due to persistent activation of the complement system. This ongoing inflammation may reduce sensitivity to anti-VEGF agents [52]. As a result, HHT demonstrates a wide range of potential applications by combining several mechanistical approaches.

Actin cytoskeleton remodelling in ECs regulated by the ROCK pathway is vital for angiogenesis. Disruptions in F-actin organisation significantly affect this process, promoting the formation of stress fibres and reducing cell migration [21]. We could show that after treatment with HHT, a significant remodelling expressed by the increase of F-actin (formation of stress fibres) within the cells occurred. This effect was completely mitigated by a preincubation with the ROCK inhibitor Y-27632, indicating a significant influence of the ROCK pathway to the observed functional effects. However, some literature suggests that this inhibitor interacts in a relatively unspecific manner with different ROCK isoforms [53]. Therefore, we went on to specifically target upstream and downstream proteins in the ROCK pathway. Surprisingly, inhibiting the upstream signalling mediator Rho with CT04 only negligible altered the effects of HHT. Other upstream regulators like Akt or FAK, regulating the phosphorylation and signalling of ROCK, were not influenced by HHT treatment as well, indicating that HHT acts through ROCK independently of upstream regulators. Inhibition of the downstream proteins LIMK1/2, myosin II and MLCK only partly reversed the anti-angiogenic actions of HHT. A Rho-independent activation of ROCK1 by caspase-3-mediated cleavage as well as ROCK2 activation by the ERM proteins did not show any effect either. This is in accordance with other studies that showed an impact of HHT on the actin rearrangement without a specific influence on the ROCK pathway: Sun et al. (2021) suggested an inhibition of the production of the extracellular matrix by fibroblasts by inhibiting the PI3K/AKT/mTOR pathway [54]. Zhang et al. (2016) showed that HHT targets myosin-9, a member of the myosin superfamily responsible for actin-based motility [55]. Porcù et al. (2023) suggested a decrease in proliferation of glioblastoma by hindering PDGFRα-dependent oncogenic signalling transduced through STAT3 and RhoA [50]. Furthermore, a relationship between the actin cytoskeleton and an efficient protein synthesis has been shown in previous research [56,57]. HHT has a well-documented capacity to inhibit mRNA translation [28,29]. The binding site of HHT at the 60S ribosomal subunit is identical with that of some other mRNA translation inhibitors, which diminish translation elongation by binding to the eukaryotic elongation factor 1 A (eEF1A) [58]. eEF1A has also been shown to interact with components of the cytoskeleton, such as actin and tubulin. Thus, it is tempting to speculate that HHT might exert its effects in part by a similar mechanism.

One further possibility to alter F-actin is the phosphorylation of HSP27 shifting the actin balance to F-actin [59,60]. HSP27 and its influence on the actin skeleton is highly correlated with the activation of p38 [41,61]. Recent findings from our group indicate that p38 can be activated by HHT in endothelial cells [31]. Consequently, the observed effects of HHT on actin dynamics may be partially attributed to this signalling pathway. p38 is known to play a significant role in angiogenesis, exhibiting both pro-angiogenic and anti-angiogenic effects in specific contexts [62–64]. Notably, sustained activation of ECs can lead to a shift in p38 MAP kinase activity from anti-angiogenic to pro-angiogenic. This suggests that the mere activation of p38 is not the sole determinant in this process, but the influence of the p38 pathway on angiogenesis highly depends on the inflammatory state of the endothelium [65,66]. Another hint in this direction is the fact that Y-27632 can effectively block the activation of p38, which might be the reason for a restoration of the HHT inhibited angiogenic effects when using Y27632 but only small effects when inhibiting the ROCK pathway specifically. It is further worth reiterating that HHT exhibits anti-inflammatory properties, which may contribute to its anti-angiogenic effects mediated through the p38 pathway [31]. It is therefore likely that – while the alteration and accumulation of filamentous actin is at least partly dependent on an enhancement of the p38/HSP27 axis – other effects of HHT contribute to the overall observed anti-angiogenic actions.

In summary, this study provides the first evidence that the FDA- and EMA-approved mRNA translation inhibitor HHT exerts anti-angiogenic effects in endothelial cells *ex vivo* and *in vitro*, at least partially due to F-actin remodelling. Inhibition of the ROCK pathway reversed these effects. Moreover, we found that the increase of F-actin is at least partly dependent on the sustained activation of p38/HSP27. Since HHT has recently been described to also exert anti-inflammatory actions, we suggest HHT as valuable approach to address pathologies that depend on inflammation-triggered angiogenesis.

Funding

This work was supported by the German Research Foundation (Deutsche Forschungsgemeinschaft, DFG) Graduate School (Graduiertenkolleg, GRK) 2336.

CRediT authorship contribution statement

Ciurus Sarah: Writing – review & editing, Formal analysis. **Dorovska Senta:** Writing – review & editing, Formal analysis. **Liu Hong:** Writing – review & editing, Formal analysis. **Zahler Stefan:** Writing – review & editing. **Fürst Robert:** Writing – review & editing, Supervision, Resources, Methodology, Funding acquisition, Conceptualization. **Völkl Matthias:** Writing – original draft, Methodology. **Burgers Luisa D.:** Writing – review & editing, Methodology, Formal analysis, Conceptualization. **Zech Thomas J.:** Writing – review & editing, Methodology, Formal analysis.

Declaration of Competing Interest

The authors declare that they have no known competing financial interests or personal relationships that could have appeared to influence the work reported in this paper.

Acknowledgements

We acknowledge the help of Mareike Lang, Isabelle Petith, Jana Peliskova and Bernadette Grohs in performing Western blot experiments.

Appendix A. Supporting information

Supplementary data associated with this article can be found in the online version at doi:10.1016/j.biopha.2025.118025.

References

[1] T.H. Adair, J.P. Montani, Integrated Systems Physiology: from Molecule to Function to Disease, in *Angiogenesis*, Morgan & Claypool Life Sciences San Rafael (CA)), 2010.
[2] C. Han, M. Barakat, L.A. DiPietro, Angiogenesis in wound repair: too much of a good thing? Cold Spring Harb. Perspect. Biol. 14 (2022) https://doi.org/10.1101/cshperspect.a041225.
[3] P. Carmeliet, Angiogenesis in life, disease and medicine, Nature 438 (2005) 932–936, https://doi.org/10.1038/nature04478.
[4] S. Kazerounian, J. Lawler, Integration of pro- and anti-angiogenic signals by endothelial cells, J. Cell Commun. Signal 12 (2018) 171–179, https://doi.org/10.1007/s12079-017-0433-3.
[5] J. Folkman, Tumor angiogenesis: therapeutic implications, N. Engl. J. Med 285 (1971) 1182–1186, https://doi.org/10.1056/nejm197111182852108.
[6] A. Fallah, et al., Therapeutic targeting of angiogenesis molecular pathways in angiogenesis-dependent diseases, Biomed. Pharm. 110 (2019) 775–785, https://doi.org/10.1016/j.biopha.2018.12.022.
[7] S.Y. Yoo, S.M. Kwon, Angiogenesis and its therapeutic opportunities, Mediat. Inflamm. 2013 (2013) 127170, https://doi.org/10.1155/2013/127170.
[8] E. Balogh, M. Biniecka, U. Fearon, D.J. Veale, Z. Szekanecz, Angiogenesis in inflammatory arthritis, Isr. Med Assoc. J. 21 (2019) 345–352.
[9] Z.L. Liu, H.H. Chen, L.L. Zheng, L.P. Sun, L. Shi, Angiogenic signaling pathways and anti-angiogenic therapy for cancer, Signal Transduct. Target Ther. 8 (2023) 198, https://doi.org/10.1038/s41392-023-01460-1.
[10] M. Potente, H. Gerhardt, P. Carmeliet, Basic and therapeutic aspects of angiogenesis, Cell 146 (2011) 873–887, https://doi.org/10.1016/j.cell.2011.08.039.
[11] R.S. Apte, D.S. Chen, N. Ferrara, VEGF in signaling and disease: beyond discovery and development, Cell 176 (2019) 1248–1264, https://doi.org/10.1016/j.cell.2019.01.021.
[12] M. Kretschmer, D. Rüdiger, S. Zahler, Mechanical aspects of angiogenesis, Cancers (Basel) 13 (2021), https://doi.org/10.3390/cancers13194987.
[13] J.M. Ebos, R.S. Kerbel, Antiangiogenic therapy: impact on invasion, disease progression, and metastasis, Nat. Rev. Clin. Oncol. 8 (2011) 210–221, https://doi.org/10.1038/nrclinonc.2011.21.
[14] S. Bellou, G. Pentheroudakis, C. Murphy, T. Fotsis, Anti-angiogenesis in cancer therapy: Hercules and hydra, Cancer Lett. 338 (2013) 219–228, https://doi.org/10.1016/j.canlet.2013.05.015.
[15] A.C. Dudley, A.W. Griffioen, Pathological angiogenesis: mechanisms and therapeutic strategies, Angiogenesis 26 (2023) 313–347, https://doi.org/10.1007/s10456-023-09876-7.
[16] N. Yadunandanan Nair, et al., Actin cytoskeleton in angiogenesis, Biol. Open 11 (2022), https://doi.org/10.1242/bio.058899.
[17] T.D. Pollard, Actin and actin-binding proteins, Cold Spring Harb. Perspect. Biol. 8 (2016), https://doi.org/10.1101/cshperspect.a018226.
[18] R. Dominguez, K.C. Holmes, Actin structure and function, Annu Rev. Biophys. 40 (2011) 169–186, https://doi.org/10.1146/annurev-biophys-042910-155359.
[19] L.D. Burgers, et al., The protein biosynthesis inhibitor vioprolide A evokes anti-angiogenic and pro-survival actions by targeting NOP14 and decreasing VEGF receptor 2- and TAZ-signaling, Biomed. Pharmacother. 152 (2022) 113174, https://doi.org/10.1016/j.biopha.2022.113174.
[20] J. Bräutigam, et al., Narciclasine inhibits angiogenic processes by activation of Rho kinase and by downregulation of the VEGF receptor 2, J. Mol. Cell Cardiol. 135 (2019) 97–108, https://doi.org/10.1016/j.yjmcc.2019.08.001.
[21] K. Riento, A.J. Ridley, Rocks: multifunctional kinases in cell behaviour, Nat. Rev. Mol. Cell Biol. 4 (2003) 446–456, https://doi.org/10.1038/nrm1128.
[22] M. Maekawa, et al., Signaling from Rho to the actin cytoskeleton through protein kinases ROCK and LIM-kinase, Science 285 (1999) 895–898, https://doi.org/10.1126/science.285.5429.895.
[23] C. Ayata, et al., Role of rho-associated kinase in the pathophysiology of cerebral cavernous malformations, Neurol. Genet 10 (2024) e200121, https://doi.org/10.1212/nxg.0000000000200121.
[24] K. Nakajima, et al., Lysophosphatidylinositol induced morphological changes and stress fiber formation through the GPR55-RhoA-ROCK pathway, Int J. Mol. Sci. 23 (2022), https://doi.org/10.3390/ijms231810932.
[25] S. Pellegrin, H. Mellor, Actin stress fibres, J. Cell Sci. 120 (2007) 3491–3499, https://doi.org/10.1242/jcs.018473.
[26] Y. Wang, et al., ROCK isoform regulation of myosin phosphatase and contractility in vascular smooth muscle cells, Circ. Res 104 (2009) 531–540, https://doi.org/10.1161/circresaha.108.188524.
[27] J. Pérard-Viret, L. Quteishat, R. Alsalim, J. Royer, F. Dumas, Cephalotaxus alkaloids, Alkaloids Chem. Biol. 78 (2017) 205–352, https://doi.org/10.1016/bs.alkal.2017.07.001.
[28] M. Fresno, A. Jiménez, D. Vázquez, Inhibition of translation in eukaryotic systems by harringtonine, Eur. J. Biochem 72 (1977) 323–330, https://doi.org/10.1111/j.1432-1033.1977.tb11256.x.
[29] M.T. Huang, Harringtonine, an inhibitor of initiation of protein biosynthesis, Mol. Pharm. 11 (1975) 511–519.
[30] V. Gandhi, W. Plunkett, J.E. Cortes, Omacetaxine: a protein translation inhibitor for treatment of chronic myelogenous leukemia, Clin. Cancer Res 20 (2014) 1735–1740, https://doi.org/10.1158/1078-0432.Ccr-13-1283.
[31] L.D. Burgers, et al., Homo-)harringtonine prevents endothelial inflammation through IRF-1 dependent downregulation of VCAM1 mRNA expression and inhibition of cell adhesion molecule protein biosynthesis, Biomed. Pharm. 176 (2024) 116907, https://doi.org/10.1016/j.biopha.2024.116907.
[32] A.A. Prome, et al., A reverse docking approach to explore the anticancer potency of natural compounds by interfering metastasis and angiogenesis, J. Biomol. Struct. Dyn. (2023) 1–16, https://doi.org/10.1080/07391102.2023.2240895.
[33] Y. Zhang, et al., Curcumin in combination with omacetaxine suppress lymphoma cell growth, migration, invasion, and angiogenesis via inhibition of VEGF/Akt signaling pathway, Front Oncol. 11 (2021) 656045, https://doi.org/10.3389/fonc.2021.656045.
[34] E.A. Jaffe, R.L. Nachman, C.G. Becker, C.R. Minick, Culture of human endothelial cells derived from umbilical veins. Identification by morphologic and immunologic criteria, J. Clin. Invest 52 (1973) 2745–2756, https://doi.org/10.1172/jci107470.
[35] L.D. Burgers, et al., The natural product vioprolide A exerts anti-inflammatory actions through inhibition of its cellular target NOP14 and downregulation of importin-dependent NF-kB p65 nuclear translocation, Biomed. Pharm. 144 (2021) 112255, https://doi.org/10.1016/j.biopha.2021.112255.
[36] M. Baker, et al., Use of the mouse aortic ring assay to study angiogenesis, Nat. Protoc. 7 (2012) 89–104, https://doi.org/10.1038/nprot.2011.435.
[37] T.J. Zech, et al., 2-Desaza-annomontine (C81) impedes angiogenesis through reduced VEGFR2 expression derived from inhibition of CDC2-like kinases, Angiogenesis 27 (2024) 245–272, https://doi.org/10.1007/s10456-024-09906-y.
[38] H. Naito, T. Iba, N. Takakura, Mechanisms of new blood-vessel formation and proliferative heterogeneity of endothelial cells, Int Immunol. 32 (2020) 295–305, https://doi.org/10.1093/intimm/dxaa008.
[39] M.H. Menhofer, et al., In vitro and in vivo characterization of the actin polymerizing compound chondramide as an angiogenic inhibitor, Cardiovasc Res 104 (2014) 303–314, https://doi.org/10.1093/cvr/cvu210.
[40] V.T. Chin, et al., Rho-associated kinase signalling and the cancer microenvironment: novel biological implications and therapeutic opportunities, Expert Rev. Mol. Med 17 (2015) e17, https://doi.org/10.1017/erm.2015.17.
[41] H.B. Sun, et al., HSP27 phosphorylation protects against endothelial barrier dysfunction under burn serum challenge, Biochem Biophys. Res Commun. 463 (2015) 377–383, https://doi.org/10.1016/j.bbrc.2015.04.152.
[42] H.M. Kantarjian, S. O'Brien, J. Cortes, Homoharringtonine/omacetaxine mepesuccinate: the long and winding road to food and drug administration approval, Clin. Lymphoma Myeloma Leuk. 13 (2013) 530–533, https://doi.org/10.1016/j.clml.2013.03.017.
[43] W. Cao, et al., Homoharringtonine induces apoptosis and inhibits STAT3 via IL-6/JAK1/STAT3 signal pathway in Gefitinib-resistant lung cancer cells, Sci. Rep. 5 (2015) 8477, https://doi.org/10.1038/srep08477.
[44] G.H. Li, et al., The small-molecule drug homoharringtonine targets HSF1 to suppress pancreatic cancer progression, Am. J. Cancer Res 14 (2024) 2072–2087, https://doi.org/10.62347/xfjh3424.
[45] X. Shi, et al., Homoharringtonine suppresses LoVo cell growth by inhibiting EphB4 and the PI3K/AKT and MAPK/EKR1/2 signaling pathways, Food Chem. Toxicol. 136 (2020) 110960, https://doi.org/10.1016/j.fct.2019.110960.
[46] X. Wang, C.C. Decker, L. Zechner, S. Krstin, M. Wink, In vitro wound healing of tumor cells: inhibition of cell migration by selected cytotoxic alkaloids, BMC Pharmacol. Toxicol. 20 (2019) 4, https://doi.org/10.1186/s40360-018-0284-4.
[47] X.J. Ye, M.F. Lin, Homoharringtonine induces apoptosis of endothelium and down-regulates VEGF expression of K562 cells, J. Zhejiang Univ. Sci. 5 (2004) 230–234, https://doi.org/10.1007/bf02840929.
[48] A. Ahmad, M.I. Nawaz, Molecular mechanism of VEGF and its role in pathological angiogenesis, J. Cell Biochem 123 (2022) 1938–1965, https://doi.org/10.1002/jcb.30344.
[49] J. Liu, et al., Homoharringtonine attenuates dextran sulfate sodium-induced colitis by inhibiting NF-κB signaling, Mediat. Inflamm. 2022 (2022) 3441357, https://doi.org/10.1155/2022/3441357.
[50] E. Porcù, et al., Identification of homoharringtonine as a potent inhibitor of glioblastoma cell proliferation and migration, Transl. Res 251 (2023) 41–53, https://doi.org/10.1016/j.trsl.2022.06.017.
[51] M. Zhu, et al., Homoharringtonine suppresses tumor proliferation and migration by regulating EphB4-mediated β-catenin loss in hepatocellular carcinoma, Cell Death Dis. 11 (2020) 632, https://doi.org/10.1038/s41419-020-02902-2.
[52] S. Yang, J. Zhao, X. Sun, Resistance to anti-VEGF therapy in neovascular age-related macular degeneration: a comprehensive review, Drug Des. Devel Ther. 10 (2016) 1857–1867, https://doi.org/10.2147/dddt.S97653.
[53] J. Kroll, et al., Inhibition of Rho-dependent kinases ROCK I/II activates VEGF-driven retinal neovascularization and sprouting angiogenesis, Am. J. Physiol. -Heart Circ. Physiol. 296 (2009) H893–H899, https://doi.org/10.1152/ajpheart.01038.2008.
[54] Y. Sun, J. Dai, R. Jiao, Q. Jiang, J. Wang, Homoharringtonine inhibits fibroblasts proliferation, extracellular matrix production and reduces surgery-induced knee

arthrofibrosis via PI3K/AKT/mTOR pathway-mediated apoptosis, J. Orthop. Surg. Res. 16 (2021) 9, https://doi.org/10.1186/s13018-020-02150-2.
[55] T. Zhang, et al., Homoharringtonine binds to and increases myosin-9 in myeloid leukaemia, Br. J. Pharmacol. 173 (2016) 212–221, https://doi.org/10.1111/bph.13359.
[56] R. Stapulionis, S. Kolli, M.P. Deutscher, Efficient mammalian protein synthesis requires an intact F-actin system, J. Biol. Chem. 272 (1997) 24980–24986, https://doi.org/10.1074/jbc.272.40.24980.
[57] S.R. Gross, T.G. Kinzy, Translation elongation factor 1A is essential for regulation of the actin cytoskeleton and cell morphology, Nat. Struct. Mol. Biol. 12 (2005) 772–778, https://doi.org/10.1038/nsmb979.
[58] A. Fan, P.P. Sharp, Inhibitors of eukaryotic translational machinery as therapeutic agents, J. Med Chem. 64 (2021) 2436–2465, https://doi.org/10.1021/acs.jmedchem.0c01746.
[59] L.K. Muranova, V.M. Shatov, N.B. Gusev, Role of small heat shock proteins in the remodeling of actin microfilaments, Biochem. (Mosc. 87 (2022) 800–811, https://doi.org/10.1134/s0006297922080119.
[60] N. Mounier, A.P. Arrigo, Actin cytoskeleton and small heat shock proteins: how do they interact? Cell Stress Chaperon-.-. 7 (2002) 167–176, https://doi.org/10.1379/1466-1268(2002)007< 0167:acashs> 2.0.co;2.
[61] S. Rousseau, F. Houle, J. Landry, J. Huot, p38 MAP kinase activation by vascular endothelial growth factor mediates actin reorganization and cell migration in human endothelial cells, Oncogene 15 (1997) 2169–2177, https://doi.org/10.1038/sj.onc.1201380.
[62] K. Issbrücker, et al., p38 MAP Kinase—a molecular switch between VEGF-induced angiogenesis and vascular hyperpermeability, FASEB J. 17 (2003) 262–264, https://doi.org/10.1096/fj.02-0329fje.
[63] I. Corre, F. Paris, J. Huot, The p38 pathway, a major pleiotropic cascade that transduces stress and metastatic signals in endothelial cells, Oncotarget 8 (2017) 55684–55714, https://doi.org/10.18632/oncotarget.18264.
[64] J.H. Park, J. Yoon, B. Park, Pomolic acid suppresses HIF1α/VEGF-mediated angiogenesis by targeting p38-MAPK and mTOR signaling cascades, Phytomedicine 23 (2016) 1716–1726, https://doi.org/10.1016/j.phymed.2016.10.010.
[65] G. Rajashekhar, et al., Pro-inflammatory angiogenesis is mediated by p38 MAP kinase, J. Cell. Physiol. 226 (2011) 800–808, https://doi.org/10.1002/jcp.22404.
[66] W. Zhou, L. Yang, L. Nie, H. Lin, Unraveling the molecular mechanisms between inflammation and tumor angiogenesis, Am. J. Cancer Res 11 (2021) 301–317.